

Numerical analyses of $\mathcal{N} = 2$ supersymmetric quantum mechanics with cyclic Leibniz rule on lattice

Daisuke Kadoh^{a,b,1}, Takeru Kamei^{c,2}, Hiroto So^{d,3}

^a Department of Physics, Faculty of Science, Chulalongkorn University, Bangkok 10330, Thailand

^b Research and Educational Center for Natural Sciences, Keio University,
Yokohama 223-8521, Japan

^c Graduate School of Science and Engineering, Ehime University, Matsuyama, 790-8577, Japan

^d Physics Department, Ehime University, Matsuyama, 790-8577, Japan

Abstract

We study a cyclic Leibniz rule, which provides a systematic approach to lattice supersymmetry, using a numerical method with a transfer matrix. The computation is carried out in $\mathcal{N} = 2$ supersymmetric quantum mechanics with the ϕ^6 -interaction for weak and strong couplings. The computed energy spectra and supersymmetric Ward-Takahashi identities are compared with those obtained from another lattice action. We find that a model with the cyclic Leibniz rule behaves similarly to the continuum theory compared with the other lattice action.

¹ kadoh@keio.jp

² kamei.ehime@gmail.com

³ hiroto.so@gmail.com

I. INTRODUCTION

The difficulty in lattice supersymmetry (SUSY) is originated from the lack of Leibniz rule [1]. Since any local lattice difference operator does not obey Leibniz rule [2, 3], it is difficult to realize the full SUSY within a local lattice theory [1, 4–6]. Several approaches in which part of SUSY is kept on the lattice and the full symmetry is restored at the continuum limit have been proposed so far [7–20]. Those are, however, the same in a sense that, without getting into details about the algebraic structure of a lattice Leibniz rule, nilpotent SUSY are realized on the lattice in various ways. The deep understanding of the lattice Leibniz rule could help us to define a lattice model naturally keeping as many symmetries as possible and to study higher dimensional SUSY theories without fine tunings, or with less fine tunings.

In Ref.[21], another type of the lattice Leibniz rule was proposed in $\mathcal{N} = 2$ SUSY quantum mechanics (QM) [22, 23], which keeps a part of symmetries exactly. The indices of the new rule appear cyclically⁴ and we refer to it as a cyclic Leibniz rule (CLR) in this paper as well as the authors of Ref.[21] did. The CLR has many solutions and the general solution for a symmetric difference operator has been studied in Ref.[24]. $\mathcal{N} = 4$ SUSY QM and $\mathcal{N} = 2$ SYK model are also defined on the lattice such that the half SUSY is exactly kept [25, 26]. For those models, the exact invariance of half symmetry naturally leads to the CLR although there is another lattice formulation with an exact symmetry in $\mathcal{N} = 2$ SUSY QM [8]. Furthermore a kind of non-renormalization theorem holds for the CLR action of the $\mathcal{N} = 4$ case such that any finite correction to the F-term is prohibited [25]. We can say that the CLR keeps various natural properties of SUSY at a perturbative level, however its non-perturbative property which will be important to extend the CLR formulations to higher dimensions is still unknown.

In this paper, we propose a lattice action with the CLR for a backward difference operator and study its non-perturbative property using numerical computations. We present a solution of the CLR for any interaction term. Numerical computations are carried out for the ϕ^6 -interaction for which SUSY is unbroken. We do not employ the standard Monte-Carlo method used in previous studies of SUSY QM [8, 17, 27–29] but a direct computational method on the basis of a transfer matrix [30, 31], see also [32–36] for related numerical methods. The obtained energy spectra show that the cut-off dependence of the CLR action

⁴ The difference between the standard Leibniz rule and the cyclic Leibniz rule is shown in section III A.

See (33) and (34) for the expressions as a product rule.

is smaller than another lattice action defined by Catterall and Gregory (CG) in Ref.[8]. Numerical results of the SUSY Ward-Takahashi identities (WTIs) also tell us that full symmetry is restored more rapidly than the CG action for the weak and strong couplings.

This paper is organized as follows. In section II, we introduce the continuum and the lattice theories of $\mathcal{N} = 2$ SUSY QM. The continuum theory is given in the Euclidean path integral formulation in section II A and the lattice theory is introduced in section II B. The CG lattice action is then presented in section II C. We formulate the CLR for the backward difference operator showing a solution for any superpotential and mention a relation between the CLR and the standard Leibniz rule in section III. Section IV presents the numerical results. In section IV A, we briefly explain the computational method based on the transfer matrix [30]. Then, using computational parameters given in section IV B, we show the numerical results of energy spectra in section IV C and those of SUSY WTIs in section IV D. We summarize in section V. Appendix A is devoted to study more about the CLR and appendix B shows the results of weak coupling expansion of several lattice actions.

II. SUSY QM AND THE LATTICE THEORY

$\mathcal{N} = 2$ supersymmetric quantum mechanics is defined in the Euclidean path integral formulation according to [22, 23, 37]. We then present a naive lattice approach to SUSY QM and introduce a known improved lattice action [8].

A. N=2 SUSY QM

With an euclidean time t , the action of $\mathcal{N} = 2$ SUSY QM is given by

$$S = \int_0^\beta dt \left\{ \frac{1}{2}(\partial_t \phi)^2 + \frac{1}{2}W^2(\phi) + \bar{\psi}\partial_t\psi + \bar{\psi}W'(\phi)\psi \right\}, \quad (1)$$

where $\phi(t)$ is a real bosonic variable and $\bar{\psi}(t), \psi(t)$ are one-component fermionic variables. Those variables satisfy the periodic boundary condition such as $\phi(\beta) = \phi(0)$. The superpotential $W(\phi)$ is any function of ϕ , which determines the physical behavior of this model. The partition function is defined as

$$Z_P = \int D\phi D\bar{\psi} D\psi e^{-S} \quad (2)$$

which is the path integral form of the Witten index.

The classical action is invariant under two SUSY transformations,

$$\begin{aligned}\delta\phi &= \epsilon\psi - \bar{\epsilon}\bar{\psi} \\ \delta\psi &= \bar{\epsilon}(\partial_t\phi - W) \\ \delta\bar{\psi} &= -\epsilon(\partial_t\phi + W),\end{aligned}\tag{3}$$

where ϵ and $\bar{\epsilon}$ are global Grassmann parameters. The Leibniz rule is needed to show that the action (1) is invariant under these transformations.

The Witten index Δ is defined by

$$\Delta \equiv \text{Tr}(e^{-\beta\hat{H}}(-1)^{\hat{F}}),\tag{4}$$

with the quantum Hamiltonian,

$$\hat{H} = \frac{1}{2}\hat{p}^2 + \frac{1}{2}W^2(\hat{q}) + \frac{1}{2}W'(\hat{q})[\hat{\psi}^\dagger, \hat{\psi}],\tag{5}$$

where \hat{q} and \hat{p} are the position and momentum operator and $\hat{\psi}^\dagger$ and $\hat{\psi}$ are the creation and annihilation operators, which satisfy $[\hat{p}, \hat{q}] = -i$ and $\{\hat{\psi}, \hat{\psi}^\dagger\} = 1$. Here $\hat{F} \equiv \hat{\psi}^\dagger\hat{\psi}$ is the fermion number operator. The trace is a summation over all possible normalized states of the system.

We can also write

$$\Delta = \text{Tr}(e^{-\beta\hat{H}_-}) - \text{Tr}(e^{-\beta\hat{H}_+}),\tag{6}$$

where $\hat{H}_\pm = \frac{1}{2}\hat{p}^2 + \frac{1}{2}W^2(\hat{q}) \pm \frac{1}{2}W'(\hat{q})$ are the Hamiltonians of bosonic ($-$) and fermionic ($+$) sectors, respectively. The Witten index does not depend on β because all non-zero eigenmodes in \hat{H}_\pm form pairs and only β -independent zero modes contribute to Δ . It is well-known that Δ is zero (non-zero) when SUSY is broken (unbroken) in this model. We study a SUSY unbroken case with $\Delta = 1$, given by $W(\phi) \simeq \lambda\phi^3$ for $|\phi| \rightarrow \infty$ in this paper.

B. Lattice theory

The lattice theory is defined on a lattice whose coordinate is given by $t = na$ ($n \in \mathbb{Z}$). Lattice bosonic and fermionic variables, which live on the sites, are expressed as ϕ_n and ψ_n , respectively. It is assumed that all variables satisfy the periodic boundary condition,

$$\phi_{n+N} = \phi_n, \quad \psi_{n+N} = \psi_n, \quad \bar{\psi}_{n+N} = \bar{\psi}_n,\tag{7}$$

where N is the lattice size with $\beta = Na$.

The difference operator ∇ acts on a lattice variable φ_n as $\nabla\varphi_n \equiv \sum_m \nabla_{nm}\varphi_m$ and its transpose is $(\nabla^T)_{nm} \equiv \nabla_{mn}$. Throughout this paper, ∇_+ and ∇_- denote a simple forward and a backward difference operator, respectively:

$$\nabla_+\varphi_n \equiv \frac{\varphi_{n+1} - \varphi_n}{a}, \quad (8)$$

$$\nabla_-\varphi_n \equiv \frac{\varphi_n - \varphi_{n-1}}{a}. \quad (9)$$

Note that $(\nabla_+)^T = -\nabla_-$.

The partition function with a lattice action S is defined by

$$Z_P \equiv \int D\bar{\psi}D\psi D\phi e^{-S}, \quad (10)$$

where

$$\int D\phi \equiv \prod_n \int_{-\infty}^{\infty} \frac{d\phi_n}{\sqrt{2\pi a}}, \quad (11)$$

$$\int D\bar{\psi}D\psi \equiv \int \prod_n d\bar{\psi}_n d\psi_n. \quad (12)$$

Here each Grassmann measure is an anti-commuting derivative as $d\psi_n \equiv \partial/\partial\psi_n$ and $d\bar{\psi}_n \equiv \partial/\partial\bar{\psi}_n$.

We now consider a naive lattice action,

$$S_{naive} = a \sum_n \left\{ \frac{1}{2}(\nabla_-\phi_n)^2 + \frac{1}{2}W^2(\phi_n) + \bar{\psi}_n \nabla_-\psi_n + \bar{\psi}_n W'(\phi_n)\psi_n \right\} \quad (13)$$

which is obtained by replacing $\phi(t), \psi(t), \bar{\psi}(t)$ and ∂_t of (1) by the corresponding lattice variables $\phi_n, \psi_n, \bar{\psi}_n$ and ∇_- and replacing the integral by the summation over lattice site. This action is not invariant under a naive lattice SUSY transformation defined by the same replacement of the variables for (3).

SUSY which is broken at $\mathcal{O}(a)$ in (13) is classically restored in the continuum limit $a \rightarrow 0$, however such a restoration does not occur at the quantum level. As seen in later sections, modifying $\mathcal{O}(a)$ interactions of the lattice action, we can keep only either one of two SUSY transformations parametrized by ϵ and $\bar{\epsilon}$ at a finite lattice spacing, and SUSY is restored in the quantum continuum limit for such a lattice model.

C. Catterall-Gregory lattice model

Before discussing the CLR, we review a lattice action proposed by Catterall and Gregory [8]:

$$S_{CG} = S_{naive} + a \sum_n \nabla_- \phi_n W(\phi_n), \quad (14)$$

where ∇_- is the backward difference operator defined in (9). Note that the added term is a kind of surface term which vanishes in the naive continuum limit.

We can show that, in the free limit given by $W(\phi) = ma\phi$, S_{CG} is invariant under the lattice SUSY transformations,

$$\begin{aligned} \delta\phi_n &= \epsilon\psi_n - \bar{\epsilon}\bar{\psi}_n \\ \delta\psi_n &= \bar{\epsilon}(\nabla_+\phi_n - W(\phi_n)) \\ \delta\bar{\psi}_n &= -\epsilon(\nabla_-\phi_n + W(\phi_n)). \end{aligned} \quad (15)$$

For interacting cases, it is not invariant under the whole transformations (15) but invariant under part of SUSY, $\delta_\epsilon = \delta|_{\bar{\epsilon}=0}$:

$$\delta_\epsilon S_{CG} = 0. \quad (16)$$

This is because the extra term of R.H.S. in (14) provides $-\delta_\epsilon S_{naive}$ for any finite lattice spacing. The remaining $\bar{\epsilon}$ symmetry in (15) is restored in the quantum continuum limit as shown in Refs.[8, 17, 27, 30] and also in section IV D of this paper.

III. CYCLIC LEIBNIZ RULE FOR BACKWARD DIFFERENCE OPERATOR

We propose an alternative lattice action with the cyclic Leibniz rule (CLR) for the backward difference operator and show a solution of the CLR for any superpotential. It is straightforward to extend the results to the case of the forward difference operator.

A. Lattice action with the CLR

The CLR for the symmetric difference operator is proposed in Ref.[21]. As a straightforward extension of Ref.[21], we introduce a lattice action with the CLR for the backward operator:

$$S_{CLR} = a \sum_n \left\{ \frac{1}{2}(\nabla_-\phi_n)^2 + \frac{1}{2}(W_n)^2 + \bar{\psi}_n \nabla_-\psi_n + \sum_m \bar{\psi}_n W'_{nm} \psi_m \right\}, \quad (17)$$

where W_n is a local function of the boson variables ⁵ and $W'_{nm} \equiv \frac{\partial W_n}{\partial \phi_m}$. We now assume that W_n satisfies the CLR,

$$\sum_n \{W_n(\nabla_-)_{nm} + \nabla_- \phi_n W'_{nm}\} = 0. \quad (18)$$

As explained in the next section, a desirable local solution is

$$W_n = \frac{U(\phi_n) - U(\phi_{n-1})}{\phi_n - \phi_{n-1}}, \quad (19)$$

where $U(\phi) = \int^\phi d\phi' W(\phi')$. The lattice action (17) classically reproduces the continuum one (1) as $a \rightarrow 0$ since $W_n = W(\phi_n) + \mathcal{O}(a)$.

The importance of CLR is understood by considering a half lattice SUSY transformation,

$$\begin{aligned} \delta_\epsilon \phi_n &= \epsilon \psi_n \\ \delta_\epsilon \psi_n &= 0 \\ \delta_\epsilon \bar{\psi}_n &= -\epsilon(\nabla_- \phi_n + W_n). \end{aligned} \quad (20)$$

The lattice action (17) with any solution of (18) is invariant under (20) because

$$\delta_\epsilon S_{CLR} = \epsilon a \sum_n X_n \psi_n = 0, \quad (21)$$

where

$$X_n \equiv - \sum_m \{W_m(\nabla_-)_{mn} + W'_{mn} \nabla_- \phi_m\} \quad (22)$$

which vanishes as long as W_n satisfies the CLR (18).

The other half transformation of $\mathcal{N} = 2$ is broken on the lattice in general, which is restored at the continuum limit as seen in section IV D. However, in the free theory, it still remains as an exact symmetry because the free lattice action with the solution (19) is invariant under

$$\begin{aligned} \delta_{\bar{\epsilon}} \phi_n &= -\bar{\epsilon} \bar{\psi}_n \\ \delta_{\bar{\epsilon}} \psi_n &= \bar{\epsilon}(\nabla_+ \phi_n - W_{n+1}) \\ \delta_{\bar{\epsilon}} \bar{\psi}_n &= 0. \end{aligned} \quad (23)$$

⁵ Note that $W_n \neq W(\phi_n)$ in general because W_n may contain ϕ_m with $m \neq n$ as long as the correlation rapidly vanishes for $|m - n| \rightarrow \infty$. See (A5) of appendix A 2 for the strict definition of the locality condition.

Note that W_{n+1} is used in $\delta_{\bar{\epsilon}}\psi_n$ instead of W_n . We can actually show that

$$\delta_{\bar{\epsilon}}S_{CLR} = \bar{\epsilon} \left\{ a \sum_n X_n \bar{\psi}_n + a \sum_{n,m} Y_{nm} (W_n \bar{\psi}_m - \bar{\psi}_m \nabla_- \phi_n) + a \sum_{nmk} Z_{nmk} \bar{\psi}_n \bar{\psi}_k \psi_m \right\}, \quad (24)$$

where

$$\begin{aligned} Y_{nm} &\equiv W'_{m,n-1} - W'_{n,m} \\ Z_{nmk} &\equiv \frac{\partial^2 W_n}{\partial \phi_k \partial \phi_m}. \end{aligned} \quad (25)$$

Although we have $X_n = 0$ from the CLR, Y_{nm} and Z_{nmk} do not vanish for a generic superpotential. However, for the free theory with the solution (19),

$$W_n = \frac{m}{2}(\phi_n + \phi_{n-1}), \quad (26)$$

it is easy to show that Y_{mn} , Z_{nmk} and (24) vanish.

B. A solution of CLR for the backward difference operators

We show that (19) is a local and well-defined solution of (18) for a generic superpotential. Once the solution is given, the lattice CLR action retains an exact SUSY as seen in the previous section.

Let us first consider the free theory. For the backward operator $(a\nabla_-)_{nm} = \delta_{nm} - \delta_{n-1,m}$, we take an ansatz solution within the nearest neighbor interactions, $W_n = d_0\phi_n + d_1\phi_{n-1} + d_2\phi_{n+1}$. It is then found that $d_0 = d_1 = 1/2, d_2 = 0$ is a solution of (18), for which (26) is obtained.

It is not easy to apply such a straightforward way to a generic superpotential. We derive another representation of (18) to find a solution. Rescaling ϕ_n of (18) as $u\phi_n$ with a parameter $u \in [0, 1]$ and using the chain rule for ∂_u , we obtain

$$\frac{\partial}{\partial u} \sum_n \{u \nabla_- \phi_n W_n |_{\phi \rightarrow u\phi}\} = 0. \quad (27)$$

Integrating (27) from $u = 0$ to $u = 1$, we find a condition that means a vanishing surface term,

$$\sum_n \nabla_- \phi_n W_n = 0. \quad (28)$$

This condition is equivalent to (18) because (18) can also be derived from (28) differentiating (28) with respect to ϕ_m .

The relation (28) is easily solved by a local function (19). All we have to do is check whether or not W_n given by (19) is a well-defined function that coincides with $W(\phi_n)$ as $a \rightarrow 0$. By integrating $\partial_u U(\phi_n - ua\nabla_- \phi_n)$ from $u = 0$ to $u = 1$ and using the chain rule for ∂_u , we have

$$U(\phi_n) - U(\phi_{n-1}) = (\phi_n - \phi_{n-1}) \int_0^1 du W(\phi_n - au\nabla_- \phi_n). \quad (29)$$

The division in (19) is well-defined because the integral of R.H.S. is well-defined for any configuration of ϕ_m . Since the integral is $W(\phi_n)$ up to $\mathcal{O}(a)$, we can immediately show that $W_n = W(\phi_n) + \mathcal{O}(a)$.

C. CLR v.s. Leibniz rule

The difference between the CLR and the standard Leibniz rule (LR) is discussed here. In the continuum theory, LR for ∂_t is $\partial_t W(\phi) = W'(\phi) \partial_t \phi$. So a naive lattice LR is introduced as

$$\text{LR} : \quad \sum_m \{ \nabla_{nm} W_m - W'_{nm} (\nabla \phi)_m \} = 0, \quad (30)$$

for W_n that is a local function of bosonic variables. Here we again use $W'_{nm} \equiv \partial W_n / \partial \phi_m$. We find that the CLR is different from LR in general since

$$\text{CLR} : \quad \sum_m \{ -\nabla_{nm}^T W_m - W'_{mn} (\nabla \phi)_m \} = 0. \quad (31)$$

Note that W' in the second term is transposed.

The CLR coincides with LR if $W'_{nm} = W'_{mn}$ for $\nabla^T = -\nabla$ (symmetric difference operators), which corresponds to the case that the lattice action is invariant under both of two SUSY transformations [21]. However, the no-go theorem [2] tells us that LR does not hold for any difference operator and any interacting cases with keeping the locality principle. It is therefore difficult to realize the full SUSY transformation exactly on the lattice. The CLR cannot be realized with a non-trivial solution in this case.

The similar argument holds for the backward difference operator ∇_- . Suppose that W_n is a solution of the CLR and $\delta_{\bar{\epsilon}} S = 0$. Using $W'_{mn} = W'_{n,m-1}$ from $Y_{nm} = 0$, we can show that the CLR coincides with LR for ∇_+ since $\nabla_-^T = -\nabla_+$ and $\sum_m W'_{mn} (\nabla_- \phi)_m = \sum W'_{nm} (\nabla_+ \phi)_m$. The no-go theorem again tells us that one cannot find a solution of the CLR so that the lattice action (17) is invariant under both of δ_ϵ and $\delta_{\bar{\epsilon}}$.

The lattice rules (30) and (31) can also be expressed as a product rule of lattice variables. As an example, let us consider a lattice superpotential,

$$W_n^{e.g.} \equiv \sum_{m,k} M_{nmk} \phi_m \phi_k, \quad (32)$$

as a discretization of $W^{e.g.}(\phi(x)) = \phi^2(x)$. Then the (two-body) LR can be expressed as

$$\sum_n \left\{ \nabla_{na} M_{bnc} - \nabla_{bn} M_{nca} + \nabla_{nc} M_{ban} \right\} = 0, \quad (33)$$

while the (two-body) CLR is

$$\sum_n \left\{ \nabla_{na} M_{nbc} + \nabla_{nb} M_{nca} + \nabla_{nc} M_{nab} \right\} = 0. \quad (34)$$

The name of *cyclic* Leibniz rule comes from a cyclicity of the indices a, b, c . In appendix A, an explicit solution for the m -body CLR is also given.

IV. NUMERICAL RESULTS

Numerical computation is carried out for the CLR action (17) with the periodic boundary conditions for the superpotential,

$$W = m\phi + \lambda m^2 \phi^3, \quad (35)$$

where λ is the dimensionless coupling constant and m is the mass. Supersymmetry is kept unbroken since the Witten index is nonzero for this potential. The energy spectra and the SUSY Ward Takahashi identities are evaluated at two coupling constants $\lambda = 0.001$ (weak) and $\lambda = 1$ (strong). We compare the results with those obtained from the CG action (14) to understand the dependence of the results on the lattice spacing.

A. Numerical methods

We begin with giving the CLR lattice action used in the actual computations:

$$S_{CLR} = a \sum_n \left\{ \frac{1}{2} (\nabla_- \phi_n)^2 + \frac{1}{2} (W_n)^2 + \bar{\psi}_n \nabla_- \psi_n + \sum_m \bar{\psi}_n W'_{nm} \psi_m \right\}, \quad (36)$$

where

$$W_n = \frac{ma}{2}(\phi_n + \phi_{n-1}) + \frac{(ma)^2\lambda}{4}(\phi_n^3 + \phi_n^2\phi_{n-1} + \phi_n\phi_{n-1}^2 + \phi_{n-1}^3), \quad (37)$$

$$W'_{nm} = \frac{ma}{2}(\delta_{nm} + \delta_{n-1,m}) + \frac{(ma)^2\lambda}{4}\{(3\phi_n^2 + 2\phi_n\phi_{n-1} + \phi_{n-1}^2)\delta_{nm} + (\phi_n^2 + 2\phi_n\phi_{n-1} + 3\phi_{n-1}^2)\delta_{n-1,m}\}. \quad (38)$$

As shown in section III A, the action (36) is invariant under a single SUSY transformation (20) thanks to the CLR (18).

The partition function and the correlation functions are expressed in terms of transfer matrices. It is straightforward to show that, integrating out the fermionic variables, the partition function (10) with (36) is given as

$$Z_P = \int D\phi \left\{ \prod_{n=1}^N (1 + A_{\phi_n\phi_{n-1}}) e^{-\mathcal{L}_{\phi_n\phi_{n-1}}} - \prod_{n=1}^N (1 - A_{\phi_{n-1}\phi_n}) e^{-\mathcal{L}_{\phi_{n-1}\phi_n}} \right\}, \quad (39)$$

where

$$A_{\alpha\beta} \equiv \frac{ma}{2} + \frac{(ma)^2\lambda}{4}(3\alpha^2 + 2\alpha\beta + \beta^2), \quad (40)$$

$$\mathcal{L}_{\alpha\beta} \equiv \frac{1}{2}(\alpha - \beta)^2 + \frac{1}{8} \left(ma(\alpha + \beta) + \frac{(ma)^2\lambda}{2}(\alpha^3 + \alpha^2\beta + \alpha\beta^2 + \beta^3) \right)^2, \quad (41)$$

because $S_B = \sum_{n=1}^N \mathcal{L}_{\phi_n\phi_{n-1}}$ and $W'_{nm} = A_{\phi_n\phi_{n-1}}\delta_{n,m} + A_{\phi_{n-1}\phi_n}\delta_{n-1,m}$. Note that $A_{\alpha\beta}$ and $\mathcal{L}_{\alpha\beta}$ are infinite dimensional matrices since $\alpha, \beta \in \mathbb{R}$.

In order to define finite dimensional matrices, each path integral measure of (39) is discretized by the Gauss-Hermite quadrature. For a function $f(x)$, the Gauss-Hermite quadrature formula is given by an approximation of the integral:

$$\int_{-\infty}^{\infty} dx f(x) \approx \sum_{x \in S_K} g_K(x) f(x), \quad (42)$$

where S_K is a set of roots of K -th Hermite polynomial H_K and the weight $g_K(x)$ is

$$g_K(x) = \frac{2^{K-1} K! \sqrt{\pi}}{K^2 H_{K-1}^2(x)} e^{x^2}. \quad (43)$$

Since K is the order of the approximation, the sum of (42) is expected to reproduce the integral of L.H.S. as $K \rightarrow \infty$.

We can express Z_P using finite dimensional matrices T_{\pm} as

$$Z_P \approx \text{tr}(T_-^N) - \text{tr}(T_+^N), \quad (44)$$

discretizing all path integral measures (11) by the quadrature:

$$\int D\phi \approx \frac{1}{(2\pi)^{N/2}} \sum_{\phi_1 \in S_K} \cdots \sum_{\phi_N \in S_K} g_K(\phi_1) \cdots g_K(\phi_N). \quad (45)$$

Here, for $\alpha, \beta \in S_K$,

$$(T_-)_{\alpha\beta} \equiv (1 + A_{\alpha\beta})R_{\alpha\beta}, \quad (46)$$

$$(T_+)_{\alpha\beta} \equiv (1 - A_{\beta\alpha})R_{\alpha\beta}, \quad (47)$$

$$R_{\alpha\beta} \equiv \sqrt{\frac{g_K(\alpha)g_K(\beta)}{2\pi}} e^{-\mathcal{L}_{\alpha\beta}}. \quad (48)$$

A comparison with (6) tells us that T_- and T_+ are a bosonic and fermionic transfer matrix, respectively. The trace of (44) means

$$\text{tr}(X) \equiv \sum_{\alpha \in S_K} X_{\alpha\alpha}, \quad (49)$$

where $X_{\alpha\beta}$ is a matrix with $\alpha, \beta \in S_K$.

Similarly, any correlation function is given in terms of the transfer matrices. We basically follow Ref.[30] to derive the expressions. The two point correlation function of the bosonic variable is

$$\langle \phi_j \phi_k \rangle \approx \frac{1}{Z} \text{Tr} \left\{ T_-^{N-k+j} D T_-^{k-j} D - T_+^{N-j+k} D T_+^{k-j} D \right\}, \quad (50)$$

for $0 \leq j \leq k \leq N$. Here D represents an operator insertion, which is defined as

$$D_{\alpha\beta} \equiv \alpha \delta_{\alpha\beta}. \quad (51)$$

The boson two-point function is exactly the same formula as that of the CG action [30]. On the other hand, the fermion two-point function is slightly different:

$$\langle \psi_j \bar{\psi}_k \rangle \approx \frac{1}{Z} \text{tr} \left\{ R T_-^{k-j-1} T_+^{N+j-k} \right\}. \quad (52)$$

for $0 \leq j \leq k \leq N$.⁶

The transfer matrices T_{\pm} can be improved by rescaling the bosonic variables before the discretization of the measures. According to Ref.[30], applying the quadrature after rescaling ϕ as $\phi \rightarrow \phi/s$ ($s \in \mathbb{R}$), we have

$$(T_-^{(s)})_{\alpha\beta} \equiv (1 + A_{\alpha\beta}^{(s)})R_{\alpha\beta}^{(s)}, \quad (53)$$

$$(T_+^{(s)})_{\alpha\beta} \equiv (1 - A_{\beta\alpha}^{(s)})R_{\alpha\beta}^{(s)}, \quad (54)$$

$$R_{\alpha\beta}^{(s)} \equiv \sqrt{\frac{g_K(\alpha)g_K(\beta)}{2\pi s^2}} e^{-\mathcal{L}_{\alpha\beta}^{(s)}}. \quad (55)$$

⁶ The formula for the CG action given in [30] is reproduced because $T_+ = R$ in the case.

where $A_{\alpha\beta}^{(s)} \equiv A_{\alpha(s)\beta(s)}$ and $\mathcal{L}_{\alpha\beta}^{(s)} \equiv \mathcal{L}_{\alpha(s)\beta(s)}$ with $\alpha(s) \equiv \alpha/s$ and $\beta(s) \equiv \beta/s$. The partition function and the correlation functions are then given by the same formulas as (44), (50) and (52) with $T_{\pm}^{(s)}$ and $R^{(s)}$ instead of T_{\pm} and R . The operator insertion D is also replaced by $D^{(s)} = D/s$. The trace is still given by (49). We can obtain computational results with a high precision by tuning the rescaling parameter s such that the Witten index $Z_P = 1$ is realized as accurate as possible.

B. Computational parameters

Table I shows the parameters used in our computations of the CLR action. We employ two representative coupling constants, $\lambda = 0.001$ as a weak coupling and $\lambda = 1$ as a strong coupling. The rescaling parameter s should be tuned for each parameter set such that the Witten index $Z_P = 1$ is reproduced as accurate as possible, as done in Ref.[30]. The matrix sizes K used for the SUSY WTI are smaller than those for the mass spectra to reduce the computational cost. This is because the SUSY WTIs are evaluated by performing the direct matrix product several times while the mass spectra are evaluated by diagonalizing T_{\pm} once. Similarly, we use the same lattice sizes with a slightly different s for the CG action.

We take $m\beta = 30$ that is large enough to obtain the numerical results with a negligible finite β effect because $e^{-\beta E_1} < O(10^{-13})$ for the first excited energy $E_1/m \geq 1$. The lattice spacing is shown as rounded numbers, which is uniquely determined from the lattice size N for fixed $m\beta$ as $ma = m\beta/N (= 30/N)$. For instance, $ma = 0.017964\dots$ for $N = 1670$ is denoted as $ma = 0.018$ in the table but we use $ma = 30/N$ in the actual computations without loss of digit.

Figure 1 shows the results of Z_P against β for several s . Although Z_P is analytically shown to be unity even on the lattice [21], the numerical results depend on β . The deviations from $Z_P = 1$ are systematic errors which come from the finite K -effect. We can decrease the errors tuning s for fixed K . We find that $s = 0.68$ leads to $|Z_P - 1| < O(10^{-9})$ for $K = 150$ in the case of $ma = 0.01$ and $\lambda = 1$. Each parameter has a different value of s so that $Z_P = 1$ is realized within $O(10^{-9})$ as shown in Table I.

$\lambda = 0.001$								$\lambda = 1$							
Energy spectra				SUSY WTI				Energy spectra				SUSY WTI			
am	s	N	K	am	s	N	K	am	s	N	K	am	s	N	K
0.020	0.47	1500	150	0.600	1.39	50	40	0.020	0.97	1500	150	0.600	2.93	50	40
0.019	0.46	1580	150	0.500	1.26	60	40	0.019	0.95	1580	150	0.500	2.68	60	40
0.018	0.45	1670	150	0.400	1.13	75	40	0.018	0.92	1670	150	0.400	2.46	75	40
0.017	0.44	1770	150	0.300	0.97	100	40	0.017	0.90	1770	150	0.300	2.08	100	40
0.016	0.42	1880	150	0.250	0.89	120	40	0.016	0.87	1880	150	0.250	1.89	120	40
0.015	0.41	2000	150	0.200	0.79	150	40	0.015	0.84	2000	150	0.200	1.69	150	40
0.014	0.40	2140	150	0.150	0.68	200	40	0.014	0.81	2140	150	0.150	1.47	200	40
0.013	0.38	2310	150	0.100	0.56	300	40	0.013	0.78	2310	150	0.100	1.18	300	40
0.012	0.37	2500	150	0.080	0.51	375	40	0.012	0.75	2500	150	0.080	1.06	375	40
0.011	0.36	2730	150	0.060	0.49	500	50	0.011	0.72	2730	150	0.060	0.91	500	40
0.010	0.34	3000	150	0.050	0.44	600	50	0.010	0.68	3000	150	0.050	0.83	600	40
0.009	0.33	3330	150	0.040	0.44	750	60	0.009	0.65	3330	150	0.040	0.74	750	40
0.008	0.33	3750	170	0.030	0.41	1000	70	0.008	0.61	3750	150	0.030	0.64	1000	40
0.007	0.30	4290	170	0.025	0.34	1200	70	0.007	0.57	4290	150	0.025	0.65	1200	50
0.006	0.27	5000	170	0.020	0.32	1500	80	0.006	0.53	5000	150	0.020	0.57	1500	50
0.005	0.27	6000	200	0.015	0.33	2000	100	0.005	0.48	6000	150	0.015	0.58	2000	70
0.004	0.24	7500	200	0.010	0.29	3000	120	0.004	0.46	7500	170	0.010	0.47	3000	70
								0.003	0.40	10000	170				
								0.002	0.32	15000	170				
								0.001	0.23	30000	200				

TABLE I. Parameters used in the numerical computations of the CLR system. Left and right tables are ones for a weak coupling $\lambda = 0.001$ and for a strong coupling $\lambda = 1$, respectively.

C. Energy spectra

The energy spectra of lattice SUSY quantum mechanics are read from two transfer matrices T_{\pm} associated with two Hamiltonians \hat{H}_{\pm} as $T_{\pm} \approx e^{-a\hat{H}_{\pm}}$. The energy eigenvalues of

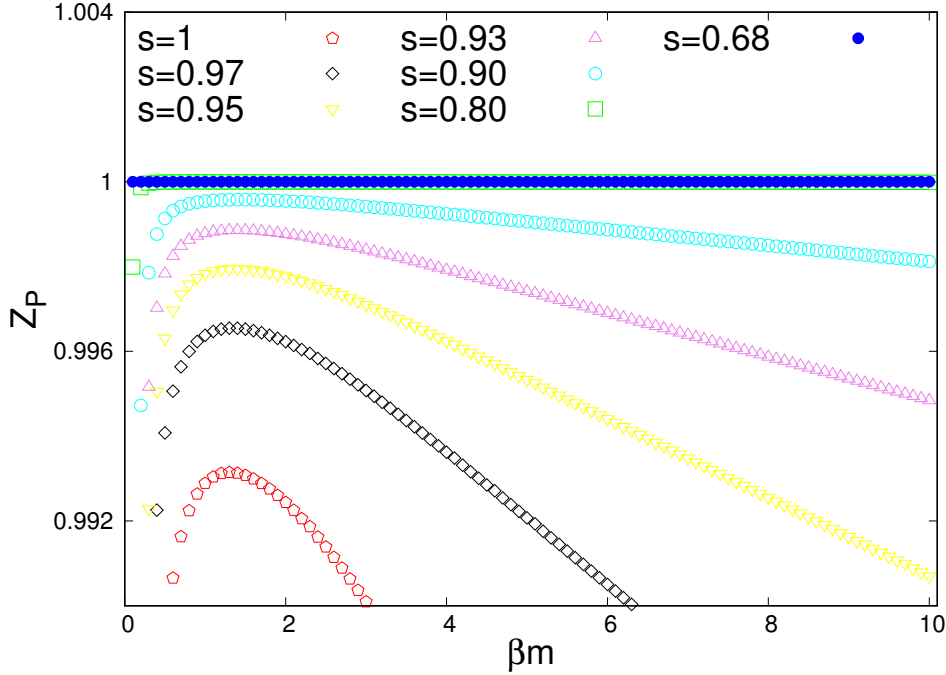


FIG. 1. Partition function with the periodic boundary condition against β for the CLR action. We use several s with fixed $K = 150$ for $ma = 0.01, \lambda = 1$.

the bosonic and fermionic states E_n^B and E_n^F are thus obtained from the n -th eigenvalue of T_{\pm} : $(T_-)_n = e^{-aE_n^B}$ and $(T_+)_n = e^{-aE_n^F}$. We use numerical diagonalizations of T_{\pm} to evaluate $(T_{\pm})_n$. The non-zero eigenvalues are degenerate between \hat{H}_+ and \hat{H}_- and only \hat{H}_- has a zero mode for the superpotential (35). We expect that T_{\pm} have the same spectra even on the lattice thanks to the exact SUSY.

1. Weak coupling results

Table II shows the ten smallest energy eigenvalues obtained from the CLR action for $\lambda = 0.001$ at a lattice spacing $ma = 0.01$. The central values are ones obtained for $K = 150$ and the errors are estimated from the largest difference among the results with $K = 140, 150, \dots, 200$. The spectra look like ones of the harmonic oscillator, $E_n = nm$ ($n = 1, 2, \dots$), since $\lambda = 0.001$ is sufficiently small. As we expected, E_n^B and E_n^F coincide with each other within the errors. The same degeneracies are observed for the other lattice spacings.

Figure 2 shows the lowest five eigenvalues against the lattice spacing ma . Since the

n	E_n^B/m	E_n^F/m
0	0.00000000001(3)	
1	1.001498936(1)	1.00149893546(2)
2	2.00598024(3)	2.005980230(1)
3	3.0134265(5)	3.01342635(3)
4	4.023822(5)	4.0238202(4)
5	5.03716(4)	5.037146(5)
6	6.0535(3)	6.05340(4)
7	7.073(1)	7.0726(2)
8	8.097(5)	8.095(1)
9	9.13(2)	9.122(5)
10	10.18(4)	10.16(1)

TABLE II. Energy eigenvalues obtained from the CLR action for $\lambda = 0.001$ at $ma = 0.01$.

difference between E_n^B and E_n^F are sufficiently smaller than the systematic errors from finite K effect, we plotted only E_n^F as E_n in the figure. As we can see, the cut-off dependence of the CLR action is milder than that of CG action.

Tables III and IV show the fit results of the lowest five energy eigenvalues for the CLR and CG actions, respectively. For the continuum extrapolation, we employ a quadratic polynomial,

$$E/m = a_0 + a_1(ma) + a_2(ma)^2. \quad (56)$$

Two actions reproduce the same a_0 , which is E_n/m at the continuum limit, within the errors. The CLR action behaves rather similar to the continuum theory in comparison with the CG action as suggested from small values of a_1 .

The weak coupling expansion of the first excited energy is demonstrated in appendix B, in which the quantum corrections to the masses are evaluated from the correlation functions. We find that, for $E_1 \equiv E_1^F = E_1^B$, the one-loop result of the CLR action is

$$\frac{E_1^{CLR}}{m} = 1 + \frac{3}{2}\lambda - \frac{1}{2}ma\lambda + O((ma)^2, \lambda^2), \quad (57)$$

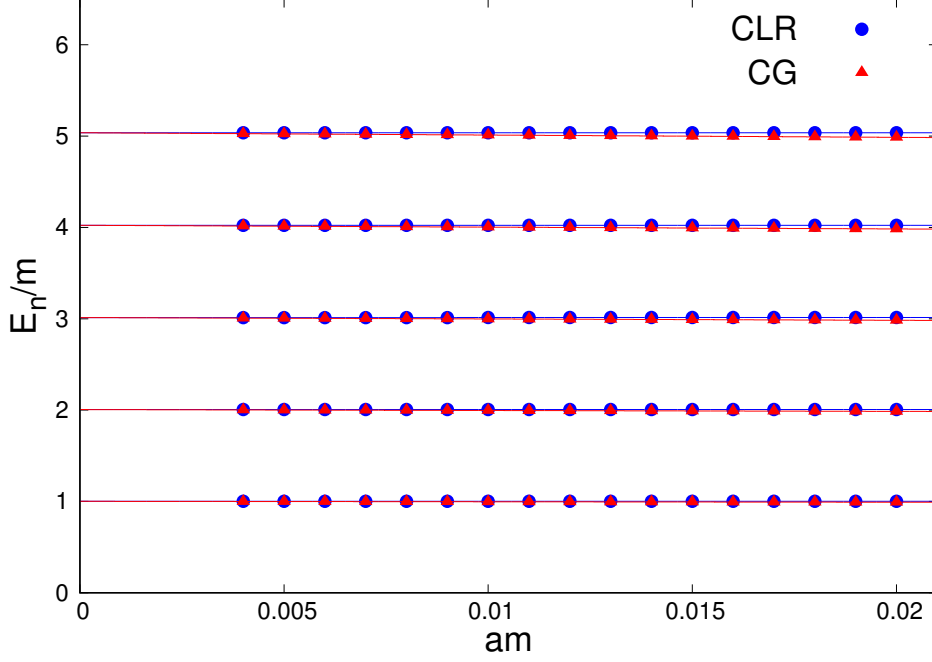


FIG. 2. Five lowest energy eigenvalues against the lattice spacing ma for $\lambda = 0.001$. The results of CLR (circles) show a better convergence than the CG results (triangles). The solid lines represent the fit results shown in Tables III and IV.

	E_1/m	E_2/m	E_3/m	E_4/m	E_5/m
a_0	1.001495535(1)	2.00597334(3)	3.0134165(4)	4.023814(4)	5.0372(4)
a_1	-0.0004999(4)	-0.00101(1)	-0.0017(2)	-0.004(2)	-0.02(2)
a_2	0.08400(4)	0.1702(9)	0.27(1)	0.5(2)	2(1)

TABLE III. Fit results of E_n for the CLR action with $\lambda = 0.001$.

	E_1/m	E_2/m	E_3/m	E_4/m	E_5/m
a_0	1.0014954(2)	2.0059732(4)	3.0134161(9)	4.023806(1)	5.037131(3)
a_1	-0.50221(6)	-1.0089(1)	-1.5202(3)	-2.0357(3)	-2.557(1)
a_2	0.330(3)	0.667(7)	1.02(2)	1.36(2)	1.8(1)

TABLE IV. Fit results of E_n for the CG action with $\lambda = 0.001$.

while one of the CG action is

$$\frac{E_1^{CG}}{m} = 1 + \frac{3}{2}\lambda - \frac{ma}{2} - \frac{1}{2}ma\lambda + O((ma)^2, \lambda^3). \quad (58)$$

Both one-loop results coincide with one of the continuum theory, $E^{cont}/m = 1 + \frac{3}{2}\lambda$, as $a \rightarrow 0$. The CG action has a large discretization error due to the third term of $O(ma)$ in (58), while the $O(a)$ -term starts from $O(\lambda ma)$ in the CLR action, which is much smaller than $O(ma)$ for $\lambda = 0.001$.

Figure 3 shows the numerical results of E_1 with the perturbative ones (57) and (58) for $ma \leq 0.02$. The numerical results nicely reproduce the perturbation theory shown by the dotted lines and the relative errors are of the order of 10^{-6} that is the same size of λ^2 . Although a linear ma dependence is seen in the CG-results, the CLR-results perfectly reproduce the continuum theory for this range of ma since the third term of (57) is negligibly small for $\lambda = 0.001$.

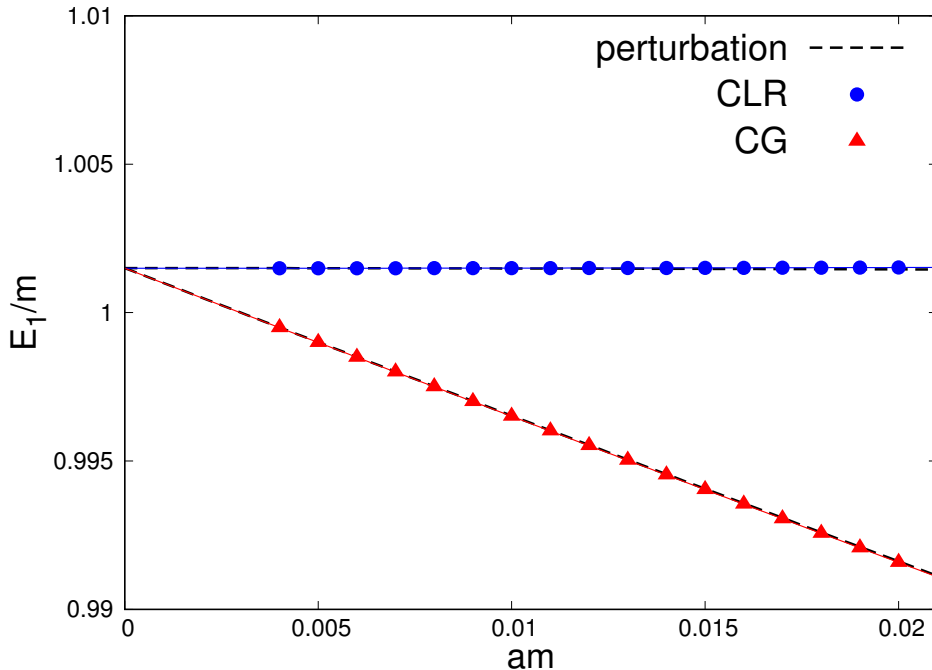


FIG. 3. Continuum limit of E_1 for $\lambda = 0.001$. The solid lines represent the fit results and the dotted lines are the perturbative results

2. Strong coupling results

Table V shows the ten smallest energy eigenvalues obtained from the CLR action for $\lambda = 1$ at a fixed $ma = 0.01$. The central values are again ones evaluated for $K = 150$ and the errors are estimated from the largest difference among the results for $K = 140, 150, \dots, 200$. The energy spectra have large quantum corrections compared to Figure II for the weak coupling $\lambda = 0.001$. E_n^B and E_n^F coincide with each other within the errors as well as the case of the weak coupling.

n	E_n^B/m	E_n^F/m
0	0.0000000000(2)	
1	1.682687275(2)	1.682687274859(4)
2	4.365387624(8)	4.36538762319(6)
3	7.62211841(4)	7.6221184119(5)
4	11.3640034(2)	11.364003389(3)
5	15.5273615(7)	15.52736144(2)
6	20.068372(3)	20.06837202(9)
7	24.954588(9)	24.9545871(4)
8	30.16073(3)	30.160725(2)
9	35.66638(9)	35.666371(6)
10	41.4546(3)	41.45459(2)

TABLE V. Energy eigenvalues obtained from the CLR action for $\lambda = 1$ at $ma = 0.01$.

Figure 4 shows the lowest five energy eigenvalues against ma for $\lambda = 1$. We also show Figure 5 which focuses on E_1 for $\lambda = 1$ for a comparison with Figure 3. The obtained E_n^F is again plotted as E_n since $E_n^F = E_n^B$ within the sufficiently small errors of $O(10^{-8})$. The cut-off dependence of the CLR action is milder than that of CG action as well as the weak coupling shown in Figure 2.

Tables VI and VII show the fit results of E_n with a quadratic function (56). The same a_0 which is E/m in the continuum limit are obtained between the CLR and CG actions. As a visible difference between Figure 2 and Figure 4 can be seen, the coefficients a_1 and a_2 are systematically larger than those for the weak coupling, which are shown in Tables III and

IV. In the strong coupling region, we can confirm that the $O(a)$ dependence of E_1 obtained for the CLR action is still smaller than that of the CG action.

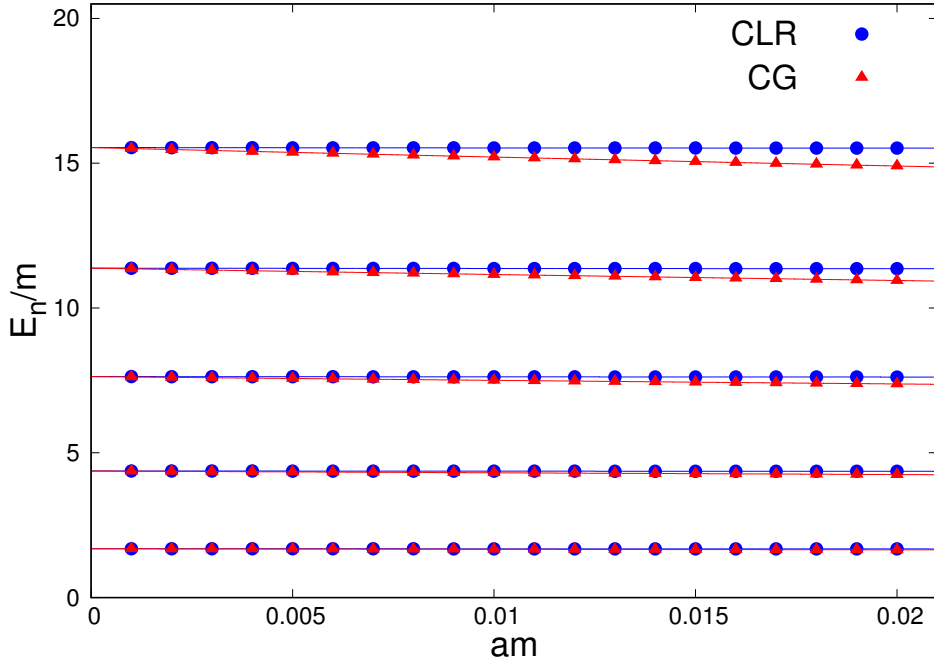


FIG. 4. Five lowest energy eigenstates against ma for $\lambda = 1$. The results of CLR and CG are shown as the circles and the triangles, respectively. The solid lines represent the fit results shown in Tables VI and VII.

	E_1/m	E_2/m	E_3/m	E_4/m	E_5/m
a_0	1.6865004(6)	4.371816(2)	7.630953(5)	11.374845(7)	15.53978(1)
a_1	-0.3907(3)	-0.684(1)	-0.985(2)	-1.282(3)	-1.575(4)
a_2	0.94(2)	4.08(8)	10.2(2)	19.8(2)	33.3(3)

TABLE VI. Fit results of E_n for the CLR action with $\lambda = 1$.

D. SUSY WT identities

The CLR action has an exact SUSY parametrized by ϵ in (20) while the other $\bar{\epsilon}$ SUSY is broken at finite lattice spacing for any interacting case. The correct mass spectra shown in

	E_1/m	E_2/m	E_3/m	E_4/m	E_5/m
a_0	1.686500(3)	4.37181(1)	7.63095(4)	11.37483(8)	15.5398(1)
a_1	-1.898(1)	-6.422(6)	-13.30(2)	-22.43(3)	-33.75(6)
a_2	3.05(9)	12.6(4)	31(1)	58(5)	95(5)

TABLE VII. Fit results of E_n for the CG action with $\lambda = 1$.

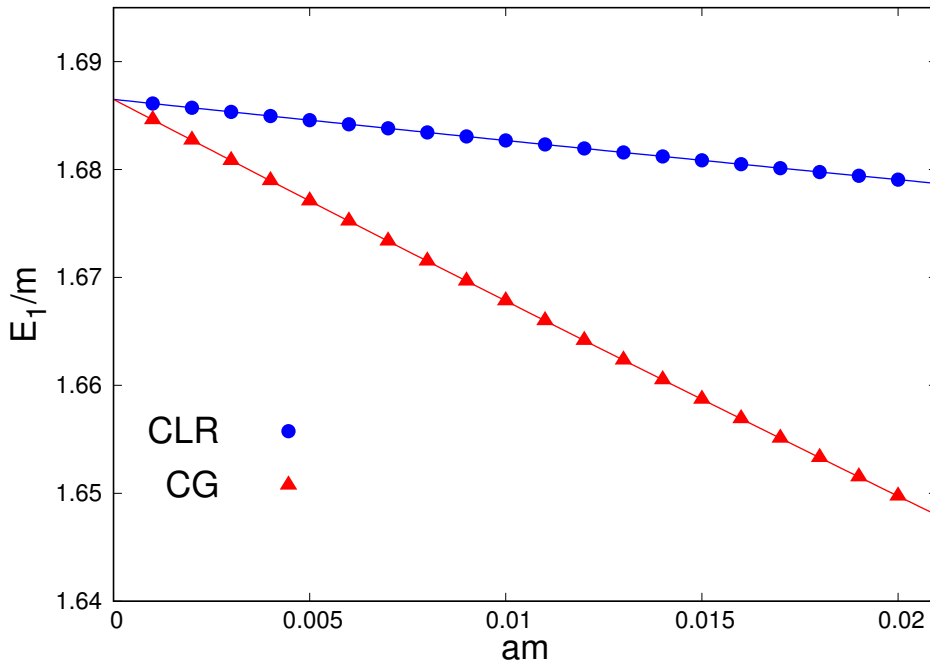


FIG. 5. Continuum limit of E_1 for $\lambda = 1$.

the previous section imply that the broken $\bar{\epsilon}$ symmetry is restored in the continuum limit. Testing the SUSY WTIs, we study the restoration of the full SUSY.

To this end, we first define the SUSY WTIs on the lattice. The broken $\bar{\epsilon}$ transformation cannot be uniquely defined on the lattice because one can add several terms that vanish in the continuum limit to the transformation. Here, for the CLR action, we employ (23) as a lattice $\bar{\epsilon}$ transformation, which is an exact symmetry in the free theory. Correspondingly, we use (15) for the CG action, whose $\bar{\epsilon}$ -transformation is exactly kept in the free case of (14).

We can show that

$$\langle \delta(\phi_n \bar{\psi}_N + \psi_n \phi_N) \rangle = \epsilon R_n + \bar{\epsilon} \bar{R}_n, \quad (59)$$

where

$$R_n \equiv \langle \psi_n \bar{\psi}_N \rangle - \langle \phi_n (\nabla_- \phi)_N \rangle - \langle \phi_n W_N \rangle, \quad (60)$$

$$\bar{R}_n \equiv \langle \psi_n \bar{\psi}_N \rangle - \langle \phi_n (\nabla_- \phi)_N \rangle - \langle W_{n+1} \phi_N \rangle, \quad (61)$$

for the CLR action. For the CG action, W_N and W_{n+1} of (60) and (61) are replaced by $W(\phi_N)$ and $W(\phi_n)$, respectively. The second term of \bar{R}_n is actually found as $\langle (\nabla_+ \phi)_n \phi_N \rangle$ which can be written as the same form as the second term of R_n using the translational invariance. Note that the third term is the only difference between R_n and \bar{R}_n .

For any interacting case, we have $R_n = 0$ since the ϵ -transformation is an exact symmetry of the lattice actions. However, \bar{R}_n does not vanish at any finite lattice spacing for the interacting cases even if it vanishes for the free theory. If the $\bar{\epsilon}$ -symmetry is restored at a quantum continuum limit, \bar{R}_n should approach zero as $a \rightarrow 0$. We evaluate \bar{R}_n numerically to confirm whether the second SUSY WTI is restored in the continuum limit or not, as already done for the CG action in Ref.[17].

Figure 6 shows $\langle \phi_n \phi_N \rangle$ and $\langle \psi_n \bar{\psi}_N \rangle$ for $\lambda = 1$ and $ma = 0.2$. When N is sufficiently large, as confirmed in the figure, $\langle \phi_n \phi_N \rangle$ and $\langle \psi_n \bar{\psi}_N \rangle$ behave as

$$\langle \phi_n \phi_N \rangle \approx C(e^{-anE_1} + e^{-a(N-n)E_1}), \quad (62)$$

$$\langle \psi_n \bar{\psi}_N \rangle \approx D e^{-anE_1}, \quad (63)$$

for $1 \ll n \ll N$. Here C and D are some constants that depend on the lattice spacing. Similarly, using the translational invariance, the other correlation functions in R_n and \bar{R}_n are expected to be

$$\langle \phi_n \nabla_- \phi_N \rangle \approx C_1(e^{-anE_1} - e^{-a(N-n-1)E_1}), \quad (64)$$

$$\langle \phi_n W_N \rangle \approx C_2 e^{-anE_1} + C_3 e^{-a(N-n-1)E_1}, \quad (65)$$

$$\langle W_{n+1} \phi_N \rangle \approx C_3 e^{-anE_1} + C_2 e^{-a(N-n-1)E_1}, \quad (66)$$

for $1 \ll n \ll N$. Here $C_1 = C(1 - e^{-aE_1})/a$ and C_2, C_3 are some constants that depend on the lattice spacing. Note that it is possible to ignore the contribution from the second excited state for $1 \ll n \ll N$. We can immediately show that

$$C_1 = C_3 = D - C_2 \quad (67)$$

from $R_n = 0$ and the second WTI holds if and only if $C_2 \rightarrow C_3$ as $a \rightarrow 0$.

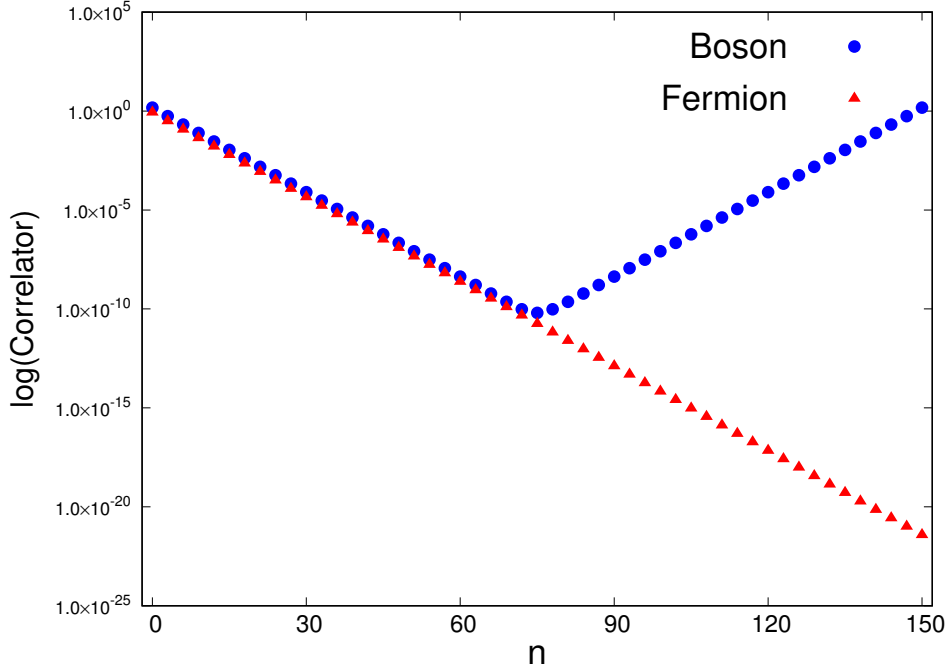


FIG. 6. $\langle\phi_n\phi_N\rangle$ and $\langle\psi_n\bar{\psi}_N\rangle$ obtained from the CLR action for $\lambda = 1$ and $ma = 0.2$. The x -axis denotes the lattice site n and the y -axis shows the numerical values of the correlators in the logarithmic scale.

Figure 7 shows the cancellation among three correlation functions in R_n (Left) and \bar{R}_n (Right) for $\lambda = 1$ and $ma = 0.2$. In Figure 8, the similar plots obtained for the CG action are shown. As we expected, the other correlators show the behavior of (64), (65) and (66). The cancellation for $n < N/2$ is realized in a different way from that of $n > N/2$. As suggested from (63)-(66), the sum of two bosonic correlators (denoted as crosses) cancels the fermion correlator (denoted as squares) for $1 \ll n \ll N/2$ while two bosonic correlators cancel each other out for $N/2 \ll n \ll N$ since the fermion correlator is approximately zero compared with the others.

Since each term of R_n and \bar{R}_n is very small for $n \simeq N/2$, we normalize them to observe the effect of the breaking term clearly:

$$S_n \equiv \frac{R_n}{|\langle\psi_n\bar{\psi}_N\rangle| + |\langle\phi_n(\nabla_-\phi)_N\rangle| + |\langle\phi_n W_N\rangle|} \quad (68)$$

$$\bar{S}_n \equiv \frac{\bar{R}_n}{|\langle\psi_n\bar{\psi}_N\rangle| + |\langle\phi_n(\nabla_-\phi)_N\rangle| + |\langle W_{n+1}\phi_N\rangle|}. \quad (69)$$

Note again that W_N and W_{n+1} of (68) and (69) are replaced by $W(\phi_N)$ and $W(\phi_n)$, respectively, for the CG action. It is immediately found that $S_n = 0$ for any n since $R_n = 0$.

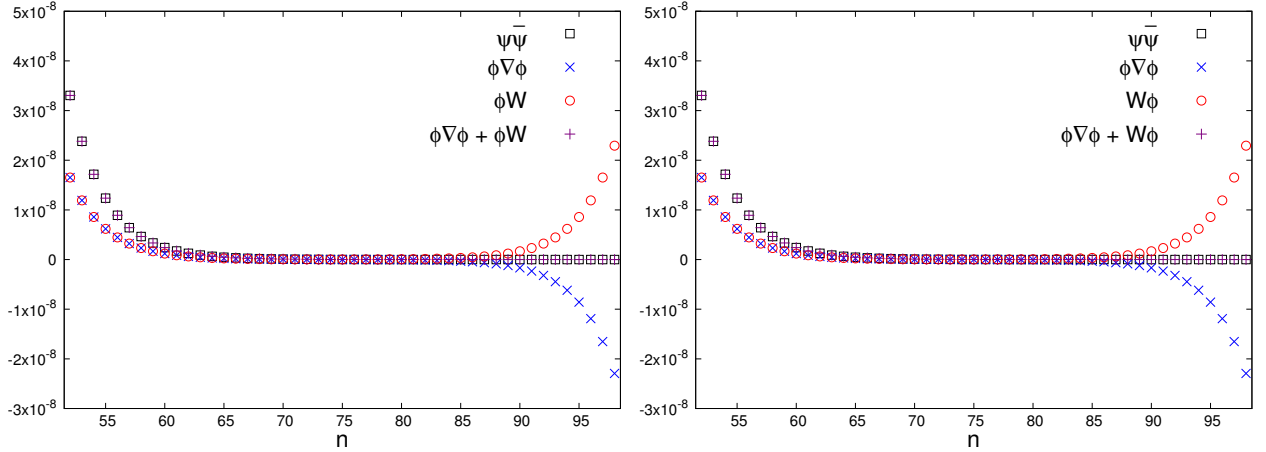


FIG. 7. Three correlation functions in R_n (left) and \bar{R}_n (right) for the CLR action. The cancellations among them are clearly observed.

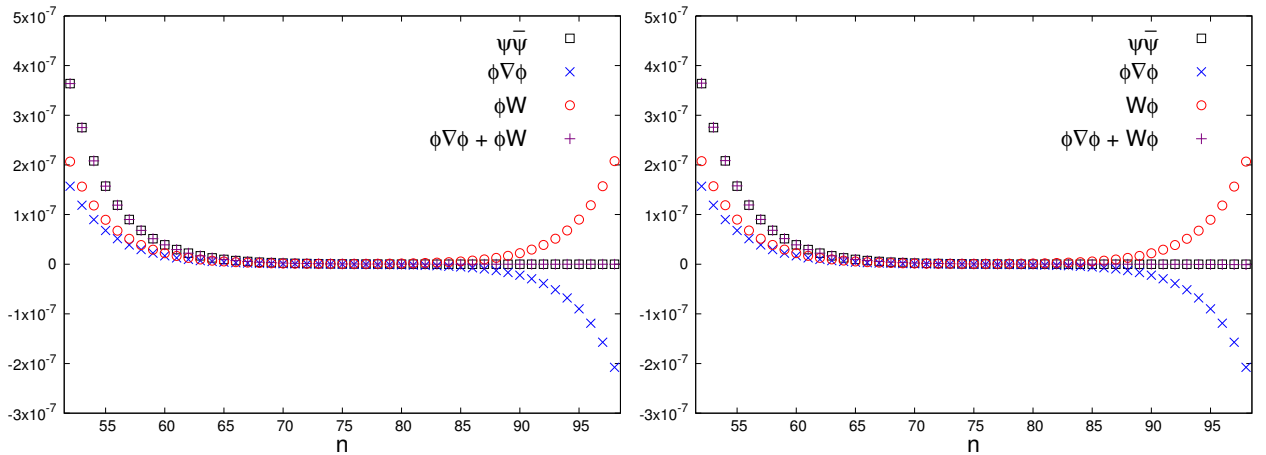


FIG. 8. Three correlation functions in R_n (left) and \bar{R}_n (right) for the CG action. The cancellations are observed as well as the CLR case shown in Figure 7.

The asymptotic behavior of \bar{S}_n can be understood from (63), (64) and (66). For sufficiently large N , it can be shown that \bar{S}_n behaves as constants:

$$S_n \approx h_1 \equiv \frac{C_2 - C_3}{2|C_3| + |D|}, \quad (1 \ll n \ll N/2) \quad (70)$$

and

$$S_n \approx h_2 \equiv \frac{C_3 - C_2}{|C_2| + |C_3|}, \quad (N/2 \ll n \ll N). \quad (71)$$

We have

$$h_2 = -2h_1 + O(h_1^2), \quad (72)$$

when C_2 and C_3 have the same sign. The similar identities as (70), (71) and (72) hold for the CG action.

In Figure 9 and Figure 10, S_n and \bar{S}_n are plotted against n . As we expected, S_n vanishes as numerical results while \bar{S}_n has two plateaux corresponding to h_1 and h_2 . We should note that the scale of the y -axis for the CLR action is rather smaller than that of the CG action. The value of \bar{S}_n rapidly changes from h_1 to h_2 around $n = N/2$ as a result of the cancellation of three correlation functions.

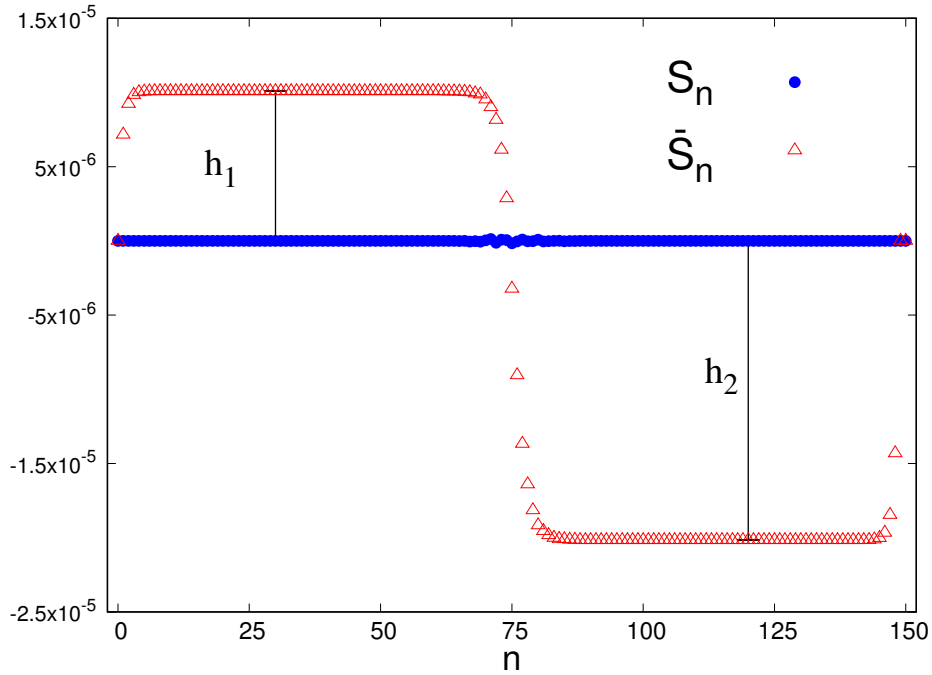


FIG. 9. S_n and \bar{S}_n for the CLR action with $\lambda = 1$ and $ma = 0.2$.

Figure 11 shows the lattice spacing dependence of h_1 and h_2 for $\lambda = 1$ and the numerical values are shown in Table VIII for the convenience of further studies. Figure 12 shows the same plot for $\lambda = 0.001$. We evaluate h_1 and h_2 at $n = N/5$ and $n = 4N/5$, respectively. It can be seen that h_1 and h_2 approach zero as $a \rightarrow 0$. Consequently, the second SUSY WTI holds in the continuum limit, that is, full SUSY is restored in the quantum continuum limit at low energy region $1 \ll n \ll N$. The breaking effect h_1 and h_2 of the CLR action are significantly smaller than the CG action even for the strong coupling. Thus we can conclude that the CLR shows a good behavior that is similar to the continuum theory at a non-perturbative level.

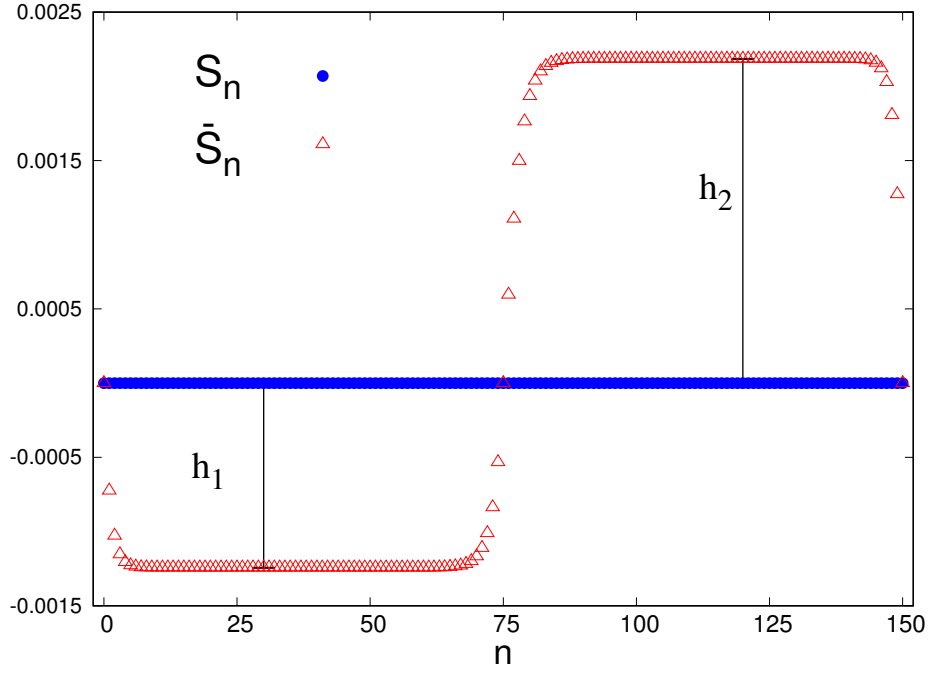


FIG. 10. S_n and \bar{S}_n for the CG action with $\lambda = 1$ and $ma = 0.2$.

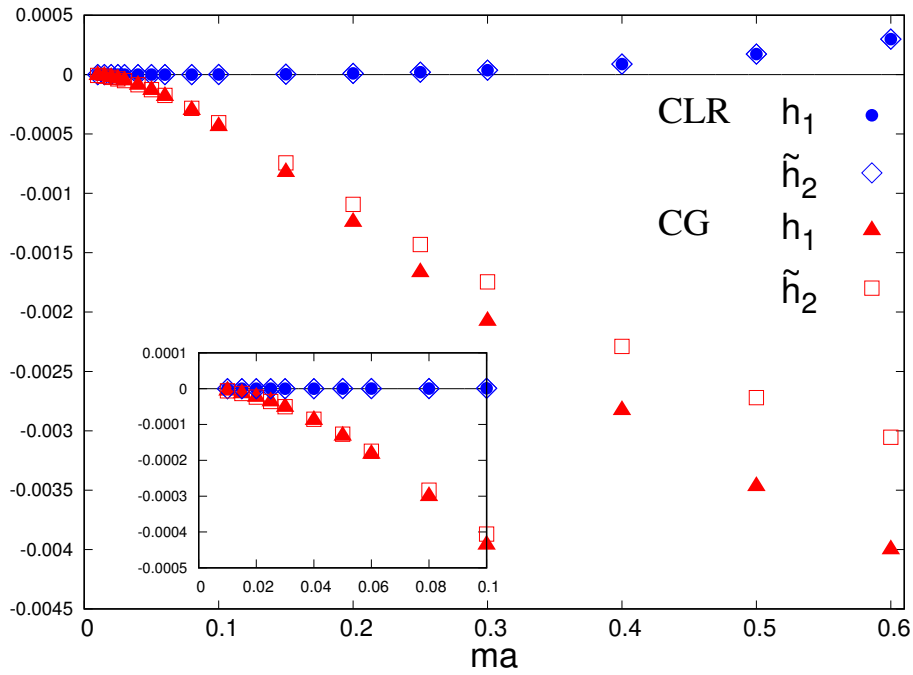


FIG. 11. Lattice spacing dependence of h_1 and h_2 for $\lambda = 1$. We plot h_1 and $\tilde{h}_2 = -h_2/2$, which are evaluated at $n = N/5$ and $n = 4N/5$, as circles and diamonds for the CLR action and triangles and squares for the CG action.

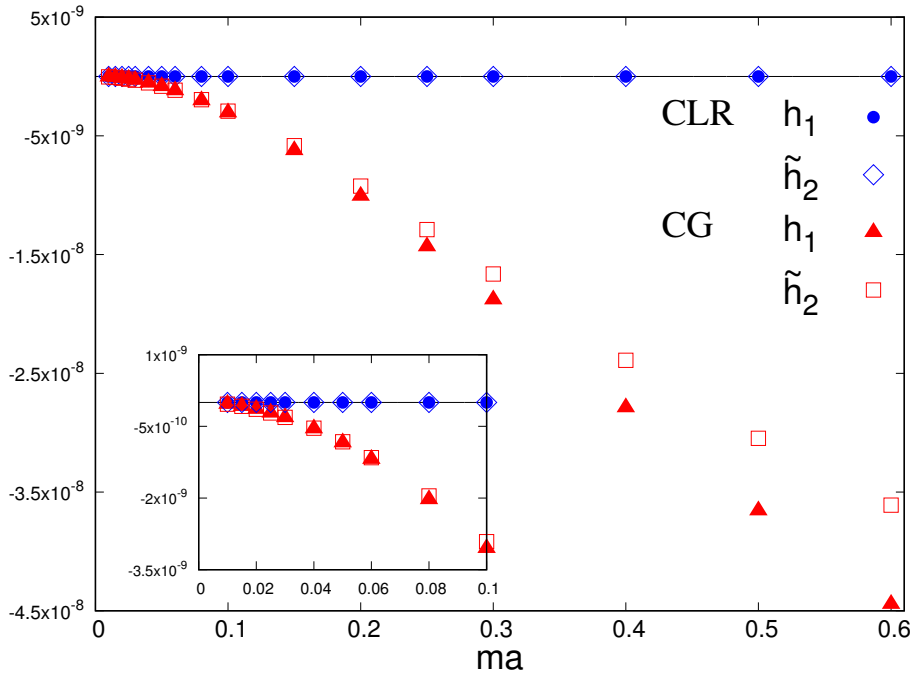


FIG. 12. Lattice spacing dependence of h_1 and h_2 for $\lambda = 0.001$. We plot h_1 and $\tilde{h}_2 = -h_2/2$, which are evaluated at $n = N/5$ and $n = 4N/5$, as circles and diamonds for the CLR action and triangles and squares for the CG action.

V. SUMMARY AND DISCUSSION

The property of the cyclic Leibniz rule has been studied in $\mathcal{N} = 2$ SUSY QM beyond the perturbation theory. We have defined the lattice action on the basis of the CLR with the backward difference operator giving a solution for any superpotential. The numerical computations have been carried out using the transfer matrix representation of the partition function and the correlation functions. Tuning the rescaling parameter, the energy spectra and SUSY Ward-Takahashi identities are obtained in a high accuracy. We have compared them with those of the Catterall-Gregory action.

Although the number of exact symmetry is the same between the CLR and the CG actions, the CLR action provides a milder cut-off dependence of energy spectra for both weak and strong couplings. In the weak coupling limit, the $\mathcal{O}(a)$ term does not appear in the energy spectra for the CLR action but does for the CG action. Even for the strong coupling, we have observed that the coefficient of $\mathcal{O}(a)$ term for the CLR action is smaller than the CG action. The lattice SUSY WTIs have shown the same tendency in the cut-off

	CLR		CG	
ma	h_1	h_2	h_1	h_2
0.600	$2.99391782(7)\times 10^{-4}$	$-5.9860435(2)\times 10^{-4}$	$-4.0012296(2)\times 10^{-3}$	$6.10759335(1)\times 10^{-3}$
0.500	$1.727581(1)\times 10^{-4}$	$-3.454565(2)\times 10^{-4}$	$-3.4686833(2)\times 10^{-3}$	$5.44024340(3)\times 10^{-3}$
0.400	$8.8385(4)\times 10^{-5}$	$-1.7675(1)\times 10^{-4}$	$-2.8283733(2)\times 10^{-3}$	$4.57824926(3)\times 10^{-3}$
0.300	$3.66716(2)\times 10^{-5}$	$-7.33404(4)\times 10^{-5}$	$-2.0775005(1)\times 10^{-3}$	$3.4908132(8)\times 10^{-3}$
0.250	$2.068870(6)\times 10^{-5}$	$-4.13765(1)\times 10^{-5}$	$-1.6669089(1)\times 10^{-3}$	$2.8615897(1)\times 10^{-3}$
0.200	$1.008226(2)\times 10^{-5}$	$-2.01643(1)\times 10^{-5}$	$-1.24342044(8)\times 10^{-3}$	$2.1858056(1)\times 10^{-3}$
0.150	$3.87190(2)\times 10^{-6}$	$-7.7438(4)\times 10^{-6}$	$-8.2362334(4)\times 10^{-4}$	$1.4866210(1)\times 10^{-3}$
0.100	$9.51290(6)\times 10^{-7}$	$-1.90258(8)\times 10^{-6}$	$-4.3652327(1)\times 10^{-4}$	$8.116901(1)\times 10^{-4}$
0.080	$4.2875(1)\times 10^{-7}$	$-8.575(1)\times 10^{-7}$	$-3.0105156(6)\times 10^{-4}$	$5.6710394(7)\times 10^{-4}$
0.060	$1.50127(2)\times 10^{-7}$	$-3.003(1)\times 10^{-7}$	$-1.8301692(4)\times 10^{-4}$	$3.495123(2)\times 10^{-4}$
0.050	$7.6345(2)\times 10^{-8}$	$-1.527(1)\times 10^{-7}$	$-1.3229006(2)\times 10^{-4}$	$2.5444813(8)\times 10^{-4}$
0.040	$3.3033(3)\times 10^{-8}$	$-6.607(1)\times 10^{-8}$	$-8.8205996(4)\times 10^{-5}$	$1.709075(1)\times 10^{-4}$
0.030	$1.1062(6)\times 10^{-8}$	$-2.21(2)\times 10^{-8}$	$-5.1741110(6)\times 10^{-5}$	$1.010147(1)\times 10^{-4}$
0.025	$5.49(2)\times 10^{-9}$	$-1.10(4)\times 10^{-8}$	$-3.6707175(4)\times 10^{-5}$	$7.19415(1)\times 10^{-5}$
0.020	$2.318(6)\times 10^{-9}$	$-4.6(1)\times 10^{-9}$	$-2.4006488(8)\times 10^{-5}$	$4.72349(1)\times 10^{-5}$
0.015	$7.56(4)\times 10^{-10}$	$-1.5(4)\times 10^{-9}$	$-1.3803022(8)\times 10^{-5}$	$2.72672(4)\times 10^{-5}$
0.010	$1.5(1)\times 10^{-10}$	$-3(1)\times 10^{-10}$	$-6.27257(1)\times 10^{-6}$	$1.24415(2)\times 10^{-5}$

TABLE VIII. Numerical values of h_1 and h_2 for $\lambda = 1$.

behavior.

In the $\mathcal{N} = 4$ case with the CLR, the number of exact SUSY is greater than the other lattice formulation. We can expect that a lattice theory with the CLR is highly improved and behaves much similar to the continuum theory. The results shown in this paper could be useful to construct the SUSY action with a modified Leibniz rule in higher dimensions.

ACKNOWLEDGMENTS

We would like to thank So Matsuura, Katsumasa Nakayama and Fumihiko Sugino for their helpful comments. This work is supported by JSPS KAKENHI Grant Numbers

Appendix A: More about the CLR

1. Solutions for other difference operators

The solution of the CLR for the forward difference operator and a symmetric difference operator $\nabla_S = \frac{1}{2}(\nabla_+ - \nabla_-)$ are presented. For any difference operator ∇ , the CLR is defined in the same manner as (31). By repeating the same procedures as in section III B, we find that (31) can be written as

$$\sum_n \nabla \phi_n W_n = 0. \quad (\text{A1})$$

It is then easy to find a local solution of (A1):

$$W_n = \begin{cases} \frac{U(\phi_{n+1}) - U(\phi_n)}{\phi_{n+1} - \phi_n} & \text{for } \nabla = \nabla_+ \\ \frac{U(\phi_{n+1}) - U(\phi_{n-1})}{\phi_{n+1} - \phi_{n-1}} & \text{for } \nabla = \nabla_S \end{cases} \quad (\text{A2})$$

The same discussions as mentioned in section III B tell us that W_n is well-defined local function that reproduces $W(\phi_n)$ up to $\mathcal{O}(a)$.

2. The m -body CLR

We now consider $W(\phi) = \sum_{m=0}^{\infty} c_m \phi^m$ with coupling constants c_m . Then the lattice superpotential W_n is also expressed as an expansion,

$$W_n \equiv \sum_{\ell=0}^{\infty} c_\ell [\phi]_n^\ell \quad (\text{A3})$$

with ⁷

$$[\phi]_n^\ell \equiv \sum_{m_1, m_2, \dots, m_\ell} M_{n, m_1, m_2, \dots, m_\ell} \phi_{m_1} \phi_{m_2} \cdots \phi_{m_\ell}, \quad (\text{A4})$$

Here we assume that $M_{n, m_1, m_2, \dots, m_\ell}$ is totally symmetric for m_1, m_2, \dots, m_ℓ except for the first index n and $[1]_n^\ell = 1$ as an overall normalization. The locality condition is strictly

⁷ The simplest example of M (but it is not a solution of CLR) is $M_{n, m_1, m_2, \dots, m_\ell} = \delta_{nm_1} \delta_{nm_2} \cdots \delta_{nm_\ell}$.

Then the lattice action (17) coincides with the naive one owing to $W_n = W(\phi_n)$ and $W'_{nm} = W'(\phi_n) \delta_{nm}$.

We can express a scattering of lattice variables around the site n by $M_{n, m_1, m_2, \dots, m_\ell}$.

defined as

$$|M_{n,m_1,m_2,\dots,m_\ell}| < C \exp\{-\rho|n - m_k|\}, \quad (\text{A5})$$

where C and $\rho > 0$ are some positive constants for $k = 1, \dots, \ell$. The summation in (A4) is well-defined because it is absolutely convergent for (A5).

The CLR in (18) is shown to be

$$\sum_n \left\{ \nabla_{nk} M_{n,n_1,n_2,\dots,n_{m-1},n_m} + \nabla_{nn_1} M_{n,n_2,n_3,\dots,n_m,k} + \dots + \nabla_{nn_m} M_{n,k,n_1,\dots,n_{m-2},n_{m-1}} \right\} = 0, \quad (\text{A6})$$

which is referred to as m -body CLR. It is easy to show that (A6) is equivalent to (18). We should note that the indices k, n_1, n_2, \dots, n_m cyclically appear in (A6). This is the reason why we called (18) the *cyclic* Leibniz rule.

The solutions of the m -body CLR for the backward difference operator can be read from (19) using

$$M_{n,m_1,m_2,\dots,m_\ell} = \frac{1}{\ell!} \frac{\partial^\ell W_n}{\partial \phi_{m_1} \partial \phi_{m_2} \dots \partial \phi_{m_\ell}} \Big|_{c_m=1, \phi=0}. \quad (\text{A7})$$

We have

$$M_{n,m} = \frac{1}{2} (\delta_{nm} + \delta_{n-1,m}), \quad (\text{A8})$$

$$M_{n,m,k} = \frac{1}{6} (2\delta_{nm}\delta_{nk} + \delta_{n-1,m}\delta_{nk} + \delta_{nm}\delta_{n-1,k} + 2\delta_{n-1,m}\delta_{n-1,k}), \quad (\text{A9})$$

$$M_{n,m,k,l} = \frac{1}{12} (3\delta_{n,m}\delta_{nk}\delta_{nl} + \delta_{n-1,m}\delta_{nk}\delta_{nl} + \delta_{nm}\delta_{n,k+1}\delta_{nl} + \delta_{nm}\delta_{nk}\delta_{n-1,l} + \delta_{n-1,m}\delta_{n-1,k}\delta_{nl} + \delta_{n-1,m}\delta_{nk}\delta_{n-1,l} + \delta_{nm}\delta_{n-1,k}\delta_{n-1,l} + 3\delta_{n-1,m}\delta_{n-1,k}\delta_{n-1,l}), \quad (\text{A10})$$

and so on.

The explicit forms of $M_{n,m_1,m_2,\dots,m_\ell}$ for the forward difference operator are ones obtained by replacing the lattice site $n - 1$ by $n + 1$ in (A8), (A9) and (A10). Those for the symmetric difference operator $\nabla_S = \frac{1}{2}(\nabla_+ + \nabla_-)$ are also obtained by the similar replacement of the lattice site.

Appendix B: Weak coupling expansion

The weak coupling expansion of the first excited energy are presented at one-loop order for the naive, the CG and the CLR actions. We perform the lattice perturbation theory

on the infinite volume lattice. The first excited energy are evaluated as effective masses obtained from the two-point correlation functions. In this section, we assume $m > 0$ and basically take $a = 1$ except for final results of the effective masses.

1. Perturbative calculation on the infinite volume lattice

The free part of a lattice action S can be expressed in the momentum space as

$$S_{\text{free}} = \int_{-\pi}^{\pi} \frac{dp}{2\pi} \left\{ \frac{1}{2} D_0^{-1}(p) \phi(p) \phi(-p) + S_0^{-1}(p) \bar{\psi}(p) \psi(-p) \right\}, \quad (\text{B1})$$

where $D_0(p)$ and $S_0(p)$ are bare propagators of the boson and the fermion, respectively. The concrete form of $D_0(p)$ and $S_0(p)$, which depends on S_{free} , are obtained by the Fourier transformation for a lattice variable φ_n :

$$\varphi(p) = \sum_{n \in \mathbb{Z}} e^{ipn} \varphi_n, \quad (\text{B2})$$

$$\varphi_n = \int_{-\pi}^{\pi} \frac{dp}{2\pi} e^{-ipn} \varphi(p), \quad (\text{B3})$$

with a useful identity $\delta_{n0} = \int_{-\pi}^{\pi} \frac{dp}{2\pi} e^{ipn}$ ($n \in \mathbb{Z}$). Note that $\varphi(p + 2\pi m) = \varphi(p)$ for $m \in \mathbb{Z}$.

The two-point correlation functions are defined as

$$D_{kl} \equiv \langle \phi_k \phi_l \rangle = \int_{-\pi}^{\pi} \frac{dp}{2\pi} D(p) e^{ip(k-l)}, \quad (\text{B4})$$

$$S_{kl} \equiv \langle \psi_k \bar{\psi}_l \rangle = \int_{-\pi}^{\pi} \frac{dp}{2\pi} S(p) e^{ip(k-l)}, \quad (\text{B5})$$

where $D(p)$ and $S(p)$ are the full propagators. We have $D_{mn} = D_{m-n,0}$ and $S_{mn} = S_{m-n,0}$ as a result of the translational invariance. The free two-point correlation functions $(D_0)_{kl}$ and $(S_0)_{kl}$ are calculated from (B4) and (B5) with $D_0(p)$ and $S_0(p)$ using the complex integral with $z = e^{ip}$.

The full propagators can be evaluated in the weak coupling expansion from D_0, S_0 and the boson and the fermion self energies Π_{kl} and Σ_{kl} . As well-known, D_{kl} is given by an infinite series,

$$D_{kl} = D_{0,kl} - (D_0 \Pi D_0)_{kl} + (D_0 \Pi D_0 \Pi D_0)_{kl} - \dots \quad (\text{B6})$$

Thus we have

$$D_{kl} = \left(\frac{1}{D_0^{-1} + \Pi} \right)_{kl}. \quad (\text{B7})$$

Similarly,

$$S_{kl} = \left(\frac{1}{S_0^{-1} + \Sigma} \right)_{kl}. \quad (\text{B8})$$

Once Π_{kl} and Σ_{kl} are evaluated at the n -loop level, D_{kl} and S_{kl} are obtained at the same order.

The effective masses m_{eff}^B and m_{eff}^F are read from the large distance behavior of D_{kl} and S_{kl} : For $|k - l| \gg 1$,

$$D_{kl} \approx C e^{-m_{\text{eff}}^B |k-l|}, \quad (\text{B9})$$

$$S_{kl} \approx C' \theta_{k,l} e^{-m_{\text{eff}}^F |k-l|}. \quad (\text{B10})$$

with

$$\theta_{k,l} \equiv \begin{cases} 1 & \text{for } k \geq l \\ 0 & \text{for } k < l. \end{cases} \quad (\text{B11})$$

At one-loop level, the self-energies provide the shifts of masses Δm in $D_0^{-1}(p)$ and $S_0^{-1}(p)$ via (B7) and (B8). The one-loop effective masses $m_{\text{eff}}^{B,F}$ are actually obtained from the formulas of tree level effective masses $m_{0,\text{eff}}^{B,F}$ with $m \rightarrow m + \Delta m$.

2. The naive action

We begin with the case of the naive action (13) whose $D_0(p)$ and $S_0(p)$ are given by

$$D_0(p) \equiv \frac{1}{2(1 - \cos p) + m^2}, \quad (\text{B12})$$

$$S_0(p) \equiv \frac{1}{1 - e^{-ip} + m}. \quad (\text{B13})$$

The free boson propagator in the position space is evaluated from (B4):

$$D_{0,kl} = \oint dz \frac{z^{k-l}}{z^2 - (m^2 + 2)z + 1}, \quad (\text{B14})$$

for $z = e^{ip}$. It is easily shown that

$$D_{0,kl} = \frac{e^{-m_{0,\text{eff}}^B |k-l|}}{2m \sqrt{1 + \frac{m^2}{4}}}, \quad (\text{B15})$$

where

$$m_{0,\text{eff}}^B = -\log \left(1 + \frac{m^2}{2} - m \sqrt{1 + \frac{m^2}{4}} \right). \quad (\text{B16})$$

Similarly,

$$S_{0,kl} = \theta_{k,l} \frac{e^{-m_{0,\text{eff}}^F |k-l|}}{1+m} \quad (\text{B17})$$

where

$$m_{0,\text{eff}}^F = \log(1+m), \quad (\text{B18})$$

and $\theta_{k,l}$ is given by (B11).

At one-loop level, the boson and fermion self energies are obtained as

$$\Pi(p) = 6\lambda m^2 \left(\frac{1}{\sqrt{1 + \frac{m^2}{4}}} - \frac{1}{1+m} \right), \quad (\text{B19})$$

$$\Sigma(p) = \frac{3\lambda m}{2\sqrt{1 + \frac{m^2}{4}}}. \quad (\text{B20})$$

The one-loop self energies provide different corrections to the mass $m \rightarrow m + \Delta m_{B,F}$ where Δm_B and Δm_F are identified from (B19) and (B20), respectively.

The one-loop effective masses are obtained by inserting $m + \Delta m_{B,F}$ into (B16) and (B18):

$$\frac{E_1^B}{m} = 1 + 3\lambda m a + \frac{(-1 - 81\lambda)m^2 a^2}{24} + O(\lambda^2, m^3 a^3) \quad (\text{B21})$$

$$\frac{E_1^F}{m} = 1 + \frac{3\lambda}{2} - \frac{(2 + 6\lambda)m a}{4} + O(\lambda^2, m^2 a^2). \quad (\text{B22})$$

We should note that E_1^B is different from E_1^F even in the continuum limit $ma \rightarrow 0$ as a result of the one-loop effect although they coincide with each other at the tree level with $\lambda = 0$.

3. The CG action

The free propagators of the CG action are

$$D_0^{CG}(p) = \frac{1}{2(1 - \cos p) + m^2 + 2m(1 - \cos p)}, \quad (\text{B23})$$

$$S_0^{CG}(p) = \frac{1}{1 - e^{-ip} + m}. \quad (\text{B24})$$

The similar calculation as done around (B14) tells us that the effective masses are degenerated as

$$m_{0,\text{eff}}^B = m_{0,\text{eff}}^F = \log(1+m), \quad (\text{B25})$$

at the tree level.

The self energies are calculated at the one-loop level as

$$\Pi(p) = \Delta m [2m + 2(1 - \cos p)], \quad (\text{B26})$$

$$\Sigma(p) = \Delta m, \quad (\text{B27})$$

where

$$\Delta m \equiv \frac{3\lambda m}{2 + m}. \quad (\text{B28})$$

These give the same correction to the boson mass and the fermion mass up to $O(\lambda)$. The one-loop effective masses are evaluated from (B25) with $m + \Delta m$. We thus obtain that

$$\frac{E_1}{m} = 1 + \frac{3\lambda}{2} - \frac{ma}{2} - \frac{\lambda(ma)^2}{2} - \frac{9\lambda(ma)^2}{4} + O(\lambda^2, (ma)^3), \quad (\text{B29})$$

for $E_1 \equiv m_{\text{eff}}^B = m_{\text{eff}}^F$ owing to an exact SUSY.

4. The CLR action

The free propagators of the CLR action are given by

$$D_0^{CLR}(p) \equiv \frac{1}{2(1 - \cos p) + m^2(1 + \cos p)/2}, \quad (\text{B30})$$

$$S_0^{CLR}(p) \equiv \frac{1}{1 - e^{-ip} + m(1 + e^{-ip})/2}. \quad (\text{B31})$$

The tree level effective masses are

$$m_{\text{eff}}^B = m_{\text{eff}}^F = \log \left(\frac{1 + \frac{m}{2}}{1 - \frac{m}{2}} \right), \quad (\text{B32})$$

which are degenerated between the boson and the fermion.

The one-loop self energies are given by

$$\Pi(p) = 2m\Delta m(1 + \cos p), \quad (\text{B33})$$

$$\Sigma(p) = \Delta m \left(\frac{1 + e^{-ip}}{2} \right), \quad (\text{B34})$$

where

$$\Delta m = \frac{\lambda m(m + 6)}{2(m + 2)}. \quad (\text{B35})$$

The one-loop effective masses are read from (B32) with $m + \Delta m$. The first excited energies for the bosonic and fermionic states are thus obtained as $E_1 \equiv m_{\text{eff}}^B = m_{\text{eff}}^F$:

$$\frac{E_1}{m} = 1 + \frac{3\lambda}{2} - \frac{\lambda ma}{2} + \frac{(ma)^2}{12} + \frac{5\lambda(ma)^2}{8} + O(\lambda^2, (ma)^3), \quad (\text{B36})$$

owing to an exact SUSY.

-
- [1] P. H. Dondi and H. Nicolai. Lattice Supersymmetry. *Nuovo Cim.*, A41:1, 1977.
 - [2] Mitsuhiro Kato, Makoto Sakamoto, and Hiroto So. Taming the Leibniz Rule on the Lattice. *JHEP*, 05:057, 2008.
 - [3] Mitsuhiro Kato, Makoto Sakamoto, and Hiroto So. Leibniz rule, locality and supersymmetry on lattice. *PoS, LATTICE2012:231*, 2012.
 - [4] Daisuke Kadoh and Hiroshi Suzuki. Supersymmetric nonperturbative formulation of the WZ model in lower dimensions. *Phys. Lett.*, B684:167–172, 2010.
 - [5] Georg Bergner. Complete supersymmetry on the lattice and a No-Go theorem. *JHEP*, 01:024, 2010.
 - [6] Keisuke Asaka, Alessandro D’Adda, Noboru Kawamoto, and Yoshi Kondo. Exact lattice supersymmetry at the quantum level for $N = 2$ Wess-Zumino models in 1- and 2-dimensions. *Int. J. Mod. Phys.*, A31(23):1650125, 2016.
 - [7] N. Sakai and Makoto Sakamoto. Lattice Supersymmetry and the Nicolai Mapping. *Nucl. Phys.*, B229:173–188, 1983.
 - [8] Simon Catterall and Eric Gregory. A Lattice path integral for supersymmetric quantum mechanics. *Phys. Lett.*, B487:349–356, 2000.
 - [9] S. Catterall and S. Karamov. A Two-dimensional lattice model with exact supersymmetry. *Nucl. Phys. Proc. Suppl.*, 106:935–937, 2002.
 - [10] Yoshio Kikukawa and Yoichi Nakayama. Nicolai mapping versus exact chiral symmetry on the lattice. *Phys. Rev.*, D66:094508, 2002.
 - [11] Andrew G. Cohen, David B. Kaplan, Emanuel Katz, and Mithat Unsal. Supersymmetry on a Euclidean space-time lattice. 1. A Target theory with four supercharges. *JHEP*, 08:024, 2003.
 - [12] Andrew G. Cohen, David B. Kaplan, Emanuel Katz, and Mithat Unsal. Supersymmetry on a Euclidean space-time lattice. 2. Target theories with eight supercharges. *JHEP*, 12:031, 2003.

- [13] Fumihiko Sugino. A Lattice formulation of superYang-Mills theories with exact supersymmetry. *JHEP*, 01:015, 2004.
- [14] Fumihiko Sugino. SuperYang-Mills theories on the two-dimensional lattice with exact supersymmetry. *JHEP*, 03:067, 2004.
- [15] Alessandro D’Adda, Issaku Kanamori, Noboru Kawamoto, and Kazuhiro Nagata. Twisted superspace on a lattice. *Nucl. Phys.*, B707:100–144, 2005.
- [16] Fumihiko Sugino. Various super Yang-Mills theories with exact supersymmetry on the lattice. *JHEP*, 01:016, 2005.
- [17] Georg Bergner, Tobias Kaestner, Sebastian Uhlmann, and Andreas Wipf. Low-dimensional Supersymmetric Lattice Models. *Annals Phys.*, 323:946–988, 2008.
- [18] Daisuke Kadoh and Hiroshi Suzuki. Supersymmetry restoration in lattice formulations of 2D $\mathcal{N} = (2, 2)$ WZ model based on the Nicolai map. *Phys. Lett.*, B696:163–166, 2011.
- [19] Daisuke Kadoh. Recent progress in lattice supersymmetry: from lattice gauge theory to black holes. *PoS*, LATTICE2015:017, 2016.
- [20] David Schaich. Progress and prospects of lattice supersymmetry. In *36th International Symposium on Lattice Field Theory (Lattice 2018) East Lansing, MI, United States, July 22-28, 2018*, 2018.
- [21] Mitsuhiro Kato, Makoto Sakamoto, and Hiroto So. A criterion for lattice supersymmetry: cyclic Leibniz rule. *JHEP*, 05:089, 2013.
- [22] Edward Witten. Dynamical Breaking of Supersymmetry. *Nucl. Phys.*, B188:513, 1981.
- [23] Edward Witten. Constraints on supersymmetry breaking. *Nucl. Phys.*, B202:253, 1982.
- [24] Daisuke Kadoh and Naoya Ukita. General solution of the cyclic Leibniz rule. *PTEP*, 2015(10):103B04, 2015.
- [25] Mitsuhiro Kato, Makoto Sakamoto, and Hiroto So. Non-renormalization theorem in a lattice supersymmetric theory and the cyclic Leibniz rule. *PTEP*, 2017(4):043B09, 2017.
- [26] Mitsuhiro Kato, Makoto Sakamoto, and Hiroto So. A lattice formulation of $\mathcal{N} = 2$ supersymmetric SYK model. 2018.
- [27] Joel Giedt, Roman Koniuk, Erich Poppitz, and Tzahi Yavin. Less naive about supersymmetric lattice quantum mechanics. *JHEP*, 12:033, 2004.
- [28] Issaku Kanamori, Hiroshi Suzuki, and Fumihiko Sugino. Euclidean lattice simulation for dynamical supersymmetry breaking. *Phys. Rev.*, D77:091502, 2008.

- [29] Christian Wozar and Andreas Wipf. Supersymmetry Breaking in Low Dimensional Models. *Annals Phys.*, 327:774–807, 2012.
- [30] Daisuke Kadoh and Katsumasa Nakayama. Direct computational approach to lattice supersymmetric quantum mechanics. *Nucl. Phys.*, B932:278–297, 2018.
- [31] Daisuke Kadoh and Katsumasa Nakayama. Lattice study of supersymmetry breaking in N=2 supersymmetric quantum mechanics. 2018.
- [32] David Baumgartner and Urs Wenger. Supersymmetric quantum mechanics on the lattice: I. Loop formulation. *Nucl. Phys.*, B894:223–253, 2015.
- [33] David Baumgartner and Urs Wenger. Supersymmetric quantum mechanics on the lattice: II. Exact results. *Nucl. Phys.*, B897:39–76, 2015.
- [34] David Baumgartner and Urs Wenger. Supersymmetric quantum mechanics on the lattice: III. Simulations and algorithms. *Nucl. Phys.*, B899:375–394, 2015.
- [35] Daisuke Kadoh, Yoshinobu Kuramashi, Yoshifumi Nakamura, Ryo Sakai, Shinji Takeda, and Yusuke Yoshimura. Tensor network formulation for two-dimensional lattice $\mathcal{N} = 1$ Wess-Zumino model. *JHEP*, 03:141, 2018.
- [36] Daisuke Kadoh, Yoshinobu Kuramashi, Yoshifumi Nakamura, Ryo Sakai, Shinji Takeda, and Yusuke Yoshimura. Tensor network analysis of critical coupling in two dimensional ϕ^4 theory. 2018.
- [37] Fred Cooper, Avinash Khare, and Uday Sukhatme. Supersymmetry and quantum mechanics. *Phys. Rept.*, 251:267–385, 1995.